JOURNAL OF THERMOPHYSICS AND HEAT TRANSFER
Vol. 18, No. 2, April–June 2004

Effect of Substrate Wettability on Frost Properties

J. L. Hoke,* J. G. Georgiadis,† and A. M. Jacobi†
University of Illinois at Urbana–Champaign, Urbana, Illinois 61801

Microscopic observations of frost deposition on clean glass (hydrophilic) and polytetrafluoroethylene (PTFE) (hydrophobic) substrates allow the quantification of frost growth and characterization of structure. In contrast to early growth behavior, the thickness of the frost layer during the mature growth increases faster on substrates that have lower contact angles, and the frost density is less than that measured for high-contact angle substrates. This behavior is explained in terms of the effects of substrate wettability and its impact on condensate distribution, the initial condition for frost growth. A higher conductivity layer is formed on the hydrophilic than on the hydrophobic substrate. Modeling that is based on a relation between thermal conductivity and frost structure is used to predict the growth rate and density on the two different substrates. These predictions agree with the experimental data and support the explanation that substrate wettability affects mature frost growth through its effect on condensate distribution at frosting incipience.

Nomenclature

A, B	=	constants [Eq. (15)]
C_p	=	condensation period, s
c_p	=	constant-pressure specific heat, J/(kg · K)
D	=	binary diffusion coefficient, m^2/s; or diameter, m
h	=	heat transfer coefficient, $W/m^2 \cdot K$
h_m	=	mass transfer coefficient, m/s
J	=	nucleation rate, $1/s \cdot m^3$
k	=	thermal conductivity, W/m · K
$\dot{m}$	=	volumetric mass deposition rate, $kg/s \cdot m^3$
P	=	probability of freezing
Re	=	Reynolds number vD/ν
T	=	temperature, K
t	=	time, s
V	=	volume, m^3
v	=	velocity, m/s
z	=	height from substrate, m
δ	=	frost height, m
ε	=	volume fraction
θ	=	contact angle
λ	=	enthalpy of sublimation of water, J/kg
ν	=	kinematic viscosity, m^2/s
ρ	=	density, kg/m^3
τ	=	dimensionless frost environmental time [see Eqs. (11) and (12)]
Ω	=	average frost spire orientation
ω	=	humidity ratio

Subscripts

a	=	air
b	=	water
D	=	diameter
eff	=	effective
f	=	frost
g	=	gas
h	=	hydraulic
i	=	initial
ice	=	ice
m	=	mature
tp	=	triple point
v	=	water vapor
w	=	solid
∞	=	freestream

Received 23 September 2002; revision received 9 September 2003; accepted for publication 23 October 2003.

*Research Engineer, Department of Mechanical and Industrial Engineering; currently Innovative Scientific Solutions, Inc., 2766 Indian Ripple Road, Dayton, OH 45440; john.hoke@wpafb.af.mil.

†Professor, Department of Mechanical and Industrial Engineering.

Introduction

THE properties of solid water depend on the scenario under which the solid is formed, its history, and present environment. Distinctive properties range from those observable by the naked eye, such as clarity and texture, to properties measured in a lab, such as atomic structure and permittivity. The desire to understand the mechanisms affecting the properties of solid water has been the basis of numerous studies[1]; however, there is still much that is unknown. This study focuses on the deposition of water on two different substrates where the environmental conditions are such that frost forms.

Frost growth can be considered to occur under two distinct scenarios: The first shall be called condensation frosting and the second ablimation frosting. The designations of condensation and ablimation, as used in this study, describe the way frost growth is initiated. In condensation frosting, water vapor deposits to form liquid droplets even at substrate temperatures well below the triple point of water. These droplets grow and coalesce with neighboring droplets. After some period, the droplets freeze and additional water vapor ablimates onto the frozen droplets, creating frost. In ablimation frosting, water vapor initially deposits on the substrate as a solid, forming the layer that continually grows through ablimation (see Ref. 2).

For condensation frosting, three regimes will be considered. The first regime is designated the condensation period. The condensation period ends, and the early frost growth period begins, when the condensate begins to freeze. The early growth period is characterized by an almost constant frost-thickness growth rate, that is, $d\delta/dt \approx$ constant. The transition from the early growth period to the mature growth period is gradual and, hence, difficult to demarcate; however, the mature growth period is characterized by an increase in thickness proportional to the square root of time, that is, $d\delta/dt \propto t^{1/2}$. The terms early and mature frost growth period are often used in the frost literature, whereas the term condensation period is sometimes referred to as a transition time. Sometimes this latter period is not distinguished at all. There are slight variations in the definitions and names used in the literature, and so it is imperative to define these terms, cf. Refs. 3–6. In Fig. 1, the structure of frost on a hydrophobic substrate is shown, corresponding to the periods

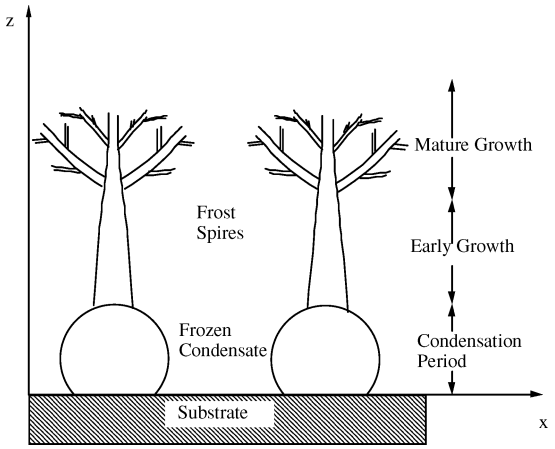

Fig. 1 Schematic of the periods of frost growth on a hydrophobic substrate.

described earlier. This research is focused on a few facets of the frosting process that have particular engineering relevance. In particular, we have studied surface wettability effects as manifested in condensate distribution and its attendant influence on the transient frost density and thickness.

There have been numerous studies reported that examine frost properties, height, density, and conductivity, as a function of environmental parameters. O'Neal and Tree[7] and Padki et al.[8] have conducted extensive reviews of the frost literature. In most of the past work, the effect of the substrate surface energy has been ignored in frosting studies, and this oversight may account for some of the scatter in frost properties reported. Recently, there have been several studies that examine the effect of substrate contact angle on frost properties. Georgiadis[9] quantified the early frost distribution on substrates of varying hydrophobicity and showed that early frost is thinner but denser on hydrophilic substrates. Dyer et al.[10] presented evidence that the trends reverse in the mature frost period, thicker and less dense on a hydrophilic substrate, in agreement with earlier findings by Seki et al.[11] The authors of these studies showed the impact that the substrate can have on frost properties, but did not examine the underlying physical mechanisms.

Methods

We hypothesize that the difference in frost-thickness growth rate observed for early and mature frost on hydrophilic and hydrophobic substrates is caused by the modification of frost structure in the condensation and early growth period. To prove this hypothesis, observations of the initiation and growth of frost were obtained on a cooled flat plate exposed to a laminar channel flow. Two substrates, polytetrafluoroethylene (PTFE) and glass, were used because of the large differences in their advancing and receding contact angles. For the ultrasonically cleaned glass, the advancing and receding contact angle were both below 10 deg and too small to measure accurately. The contact angles on the PTFE, as cleaned by the test protocol, were 103 and 84 deg for the advancing and receding contact angles with a 1.8- and 3.4-deg standard deviation, respectively. The test sections were incorporated in two separate wind tunnels. The first wind tunnel had a flow section cross section of 3 by 18 mm and was attached to the stage of a scanning confocal microscope; near-micrometer resolution images of the incipient frost were acquired. Most of the incipient frost experiments were conducted at constant air and substrate temperature conditions ($\pm 0.4^{\circ}$C) with an airflow bulk velocity of approximately 0.93 m/s (Re_{D_h} of $367 \pm 5\%$).

The procedure for examining the frost in the early growth period began with conditioning the substrate. The glass substrate used was a glass coverslip approximately 0.25 mm in thickness, and the PTFE substrate was 0.05 mm of PTFE attached to a 0.25-mm-thick piece of aluminum by 0.04 mm of adhesive. The glass substrate was ultrasonically cleaned for 5 min in a detergent bath held at 50°C, followed by a deluge of water and then de-ionized water. The substrate was then ultrasonically cleaned in de-ionized water for 5 min at 50°C, followed by a rinse of de-ionized water. The glass substrate was dried on a hotplate at 300°C. The cleaning procedure for the PTFE was much simpler and consisted of wiping the surface with a soft cloth and ethyl alcohol. In the experiments conducted to examine the early growth period, the substrate was discarded after each experiment.

After the cleaning procedure, the substrate was placed in the test section. A thin layer of thermal paste was used under the substrate to ensure thermal contact. Dry nitrogen was circulated through the wind tunnel while the substrate was being cooled to the desired temperature. The cooling of the substrate was achieved by pumping the vapor from a tank of liquid nitrogen through an aluminum heat exchanger under the substrate. A proportional–integral–derivative (PID) controller was used to control the temperature of the substrate via heaters inserted in the liquid nitrogen. Once the desired conditions were reached, the flow through the wind tunnel was switched from the dry nitrogen to air conditioned to the desired humidity. The temperature of the substrate was, therefore, constant during the entire early growth period. Images of the condensation and early frost growth were acquired at 30 frames/s. The condensation period began at the appearance of the first droplets and ended when the droplets froze. Freezing was evident by a change in the light reflected from the droplets. The error in measuring the condensation period was ± 1 s.

A larger wind tunnel with a test cross-sectional area of 13 by 51 mm was used to observe frost during the mature growth period. The substrate preparation procedure for the glass that was used in the early growth study could not be repeated because of the size of the substrates required. Instead, a soft cloth and ethyl alcohol were used to clean both the PTFE and the glass. This resulted in an advancing and receding contact angle of water on the glass of 40 and 29 deg (and a standard deviation of 6.3 and 4.6 deg), respectively, whereas the contact angle for the PTFE was the same as that in the early growth period because the cleaning procedure was identical to that performed for the early growth study. The substrate was placed in the wind tunnel flush with the adjoining sections. A thermal paste was used to ensure thermal contact with an aluminum heat exchanger through which a chilled solution of ethylene glycol and water flowed. The humidity and air temperature of this recirculating wind tunnel were allowed to come to steady state approximately 2 h before the chilled solution was pumped through the aluminum heat exchanger under the test substrate. The thickness of the frost was measured every 500 s to ± 0.1 mm by a laser sheet imaging technique. In the early growth period, the error in height measurement was higher, being ± 0.3 mm. The mass of frost deposited on a small section of the substrate was measured by removing a 51 by 102 mm section of the substrate and weighing it on a balance, accurate to ± 0.0005 g. The section of frost removed was located 75–176 mm downstream from the leading edge of the chilled portion of the wind tunnel. The uncertainty in the temperatures reported is $\pm 0.2^{\circ}$C, whereas the uncertainty in the absolute humidity reported is 0.3 g/kg. The flow in the tunnel was considered to be fully developed channel flow with a development length of 31 hydraulic diameters upstream of the test section. The turbulence intensity was measured to be less than 2.5% at an average air velocity of 1 m/s. Further details of the micro- and macroscopic experimental setups were given by Georgiadis et al.,[12] Dyer et al.,[10] and Hoke et al.[2]

Experimental Results and Observations

The emphasis of the present study was placed on bridging the scale between the early and mature frost growth by extension of the confocal study and by careful characterization of the substrates. First, the condensation period and then the early frost growth period were examined with the scanning confocal microscope. For two separate experiments, the condensate on the substrate was reconstructed in a three-dimensional image to show differences in condensate distribution. A reconstruction of the condenstate on the substrate immediately preceding the freezing event (0.30 second before freezing) is shown in Fig. 2. The image on the left side of Fig. 2 was reconstructed by the measurement of the location and diameter

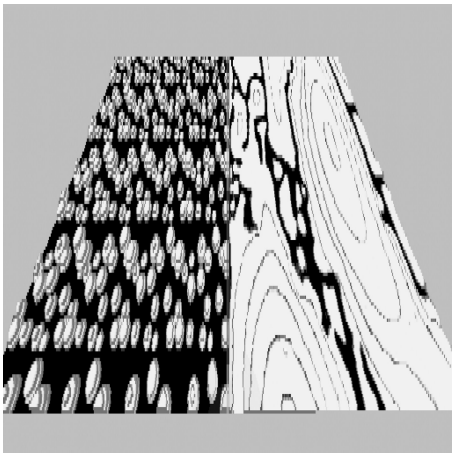

Fig. 2 Reconstruction of initial condensation on PTFE (left) and glass (right) substrates, immediately preceding freezing, showing significant difference in water distribution for PTFE conditions ($T_w = -10.2°C$, $T_a = -0.24$, and $\omega = 0.003$) and glass conditions [$T_w = -11.4°C$, $T_a = -1.24$, and $\omega = 0.002$ (peak height of condensate shown in Fig. 3, $v = 0.93$ m/s)].

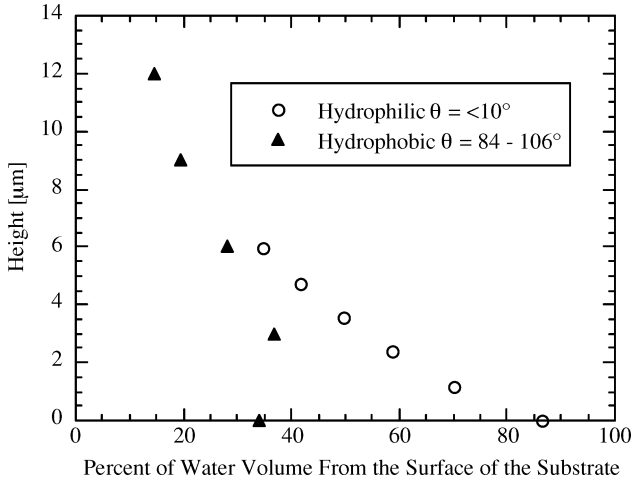

Fig. 3 Volume fraction of water between the substrate and a plane above the substrate; hydrophobic and hydrophilic volume fraction error is ±15 and ±5%, and the error in peak height was ±1 and ±0.3 μm, respectively (conditions the same as Fig. 2).

of each droplet in the field of view of the scanning confocal microscope and under the assumption that the contact angle was that of the advancing contact angle. The image on the right was created when the perimeter of each of the interference fringes created by the confocal microscope were traced and it was realized that each fringe demarks an increase in the droplet thickness of one-half the laser wavelength. With this information, density and water distribution above the substrate can be calculated. The confocal microscope used a 632-nm wavelength laser. On the hydrophobic substrate, the condensate was approximately two times higher than on the hydrophilic substrate, whereas the estimated density of condensate on the hydrophobic substrate was approximately 42% of that on the hydrophilic substrate. Water was seen to cover 86% of the hydrophilic substrate surface area but only 34% that of the hydrophobic substrate. The volume fraction between a plane above the substrate and the surface of the substrate is shown in Fig. 3, vs the height of the imaginary plane above the substrate. Note that at zero height, the value was equivalent to the substrate surface area coverage and that at the maximum height shown, the value is that of the density of the entire layer. The shape of the curves, shown in Fig. 3, depends on the contact angle on the different substrates. The conditions for these two experiments were similar: a substrate temperature of −10.2 and −11.4°C, an air temperature of −0.24 and −1.24°C, an airflow rate of 0.93 m/s, and an absolute humidity of 0.003 and 0.002 for the

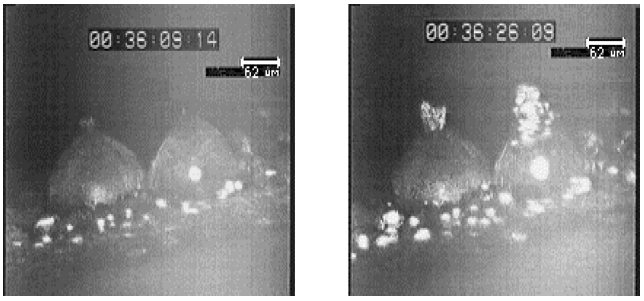

Fig. 4 Frost spires emerging from frozen droplets on hydrophobic PTFE: $T_w \sim -13°C$, $T_a \sim 21°C$, $\omega \sim 0.006$, $v = 0$, and time ∼ 300 s.

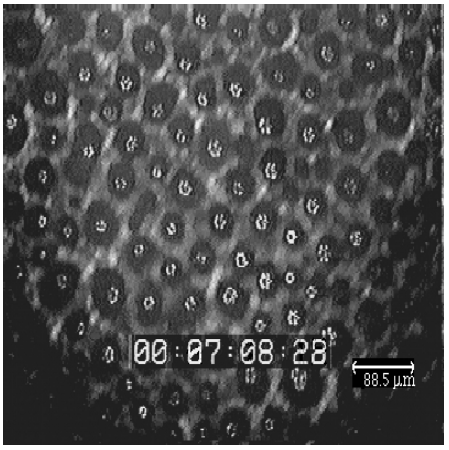

Fig. 5 Frost spires are evident from the center of each droplet: $T_w \sim -13°C$, $T_a \sim 11°C$, $\omega \sim 0.005$, $v = 0.93$ m/s, and time ∼ 400 s.

hydrophobic and hydrophilic substrate, respectively. The condensation periods for these two tests were also similar: 300 s for the PTFE substrate and 270 s for the glass substrate.

As will be seen, the distribution of water on the substrate at the end of the condensation period significantly affects the conductivity of the frost layer. The substrate contact angle was shown to have a significant effect on the distribution of water at the end of the condensation period (refer to Fig. 2); however, the substrate temperature and absolute humidity also affect the distribution. For example, lower substrate temperatures typically result in smaller, more numerous droplets.[2] There exist substrate temperature and absolute humidity conditions that reduce the influence of the substrate contact angle, for example, when either a sparse amount of water forms on the substrate or when the substrate is flooded at the end of the condensation period; the contact angle has little or no influence on the distribution of liquid.

When the condensation period ends, the freezing front propagates quickly and continuously across the hydrophilic substrate,[12] but it progresses from droplet to droplet in discrete steps across the hydrophobic substrate. See Ref. 9 for a detailed description of this event. Water ablimates onto the frozen water droplets, and the familiar structure of frost begins to appear. However, there are significant differences in the growth patterns of the frost that forms on the spherical-shaped, frozen droplets of the hydrophobic substrate and the layer of ice on the hydrophilic substrate.[2]

In Fig. 4, frost spires emerging from the top of a frozen droplet on hydrophobic PTFE are shown. Looking down on the droplets, a frost spire emerging from the center of each droplet is evident in Fig. 5. It is obvious from Fig. 5 that the density of the initial frost layer is dependent on the number and distribution of droplets on the substrate. In Fig. 5, the volume fraction of the crystals growing up from the droplets is approximately 5%, based on the light reflected from the growing spires.

On the hydrophilic substrate, the condensation period ends abruptly as the freezing front propagates quickly through the thin

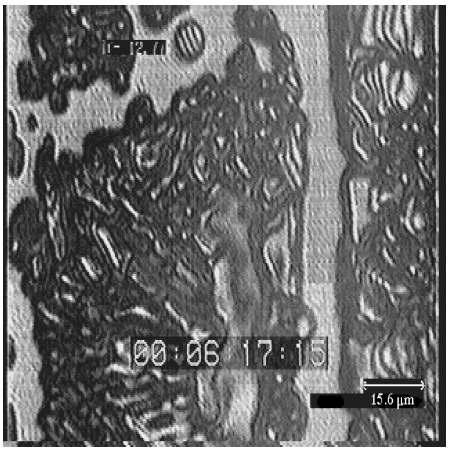

Fig. 6 Ice distribution and crystal boundaries observed on a hydrophilic substrate immediately after the freezing event: $T_w \sim -13°C$, $T_a \sim 11°C$, $\omega \sim 0.005$, $v = 0.93$ m/s, and time ~ 360 s.

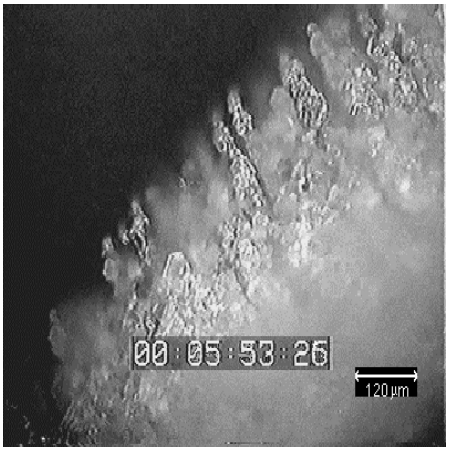

Fig. 7 Crystal growth on a hydrophilic substrate: $T_w \sim -13°C$, $T_a \sim 21°C$, $\omega \sim 0.006$, $v = 0$, and time ~ 340 s.

liquid film covering the substrate. Figure 6 shows the frozen condensate on a hydrophilic substrate. There were many different crystals in various crystallographic orientations evident in Fig. 6. In contrast to the frost growth that occurs on the protrusion formed on the frozen condensate appearing on the hydrophobic substrate, frost grown on the hydrophilic substrate has many possible locations to initiate growth and densify. A side view of the crytals on a hydrophilic substrate is shown in Fig. 7.

The temperature of the substrate can also dramatically affect the early growth. Shown in Fig. 8 is the early growth of frost on PTFE at three different subtrate temperatures. In Fig. 8a at a substrate temperature of $-11°C$ there are approximately 30 independent spires growing up from the frozen condensate, whereas in Figs. 8b and 8c there are more than 70 and more than 200 at substrate temperatures of -17.5 and $-25.1°C$, respectively. At lower substrate temperatures, the number of crystals evident in the images increases, whereas the diameter of these crystals decreases.

The frost thickness as a function of time for frost grown on two different substrates is shown in Fig. 9. The hydrophilic substrate is glass with a water-advancing contact angle of 40 deg and a receding contact angle of 29 deg, whereas the hydrophobic substrate was PTFE with an advancing contact angle of 106 deg and a receding contact angle of 84 deg. The average air velocity for both tests was 1.2 m/s. The frost grown on the hydrophilic substrate is shown to have grown over 25% thicker after 3500 s than the frost grown on the hydrophobic substrate. There was, however, a difference of approximately 500 s in the condensation period for these two substrates. When the frost height on the hydrophobic substrate at 3500 s is compared to the height of frost on the hydrophilic substrate at 3000 s, the difference in the duration of condensation can be removed. With a correction for the condensation period taken into account, frost on the hydrophilic substrate was still 23% thicker than that on the hydrophobic substrate. The density of the frost grown on the hydrophilic substrate was 14% lower than that on the hydrophobic substrate (the uncertainty in the density measurement was 5.8 and 7% for frost grown on the hydrophilic and hydrophobic substrates, respectively).

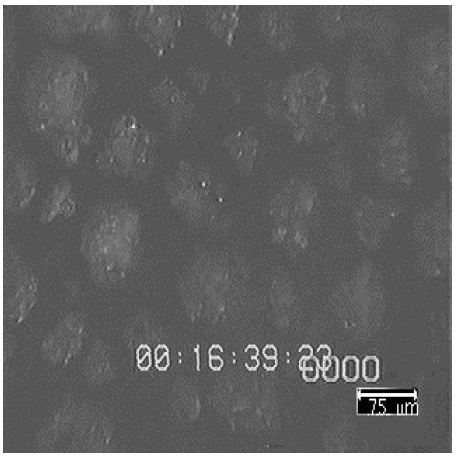

a)

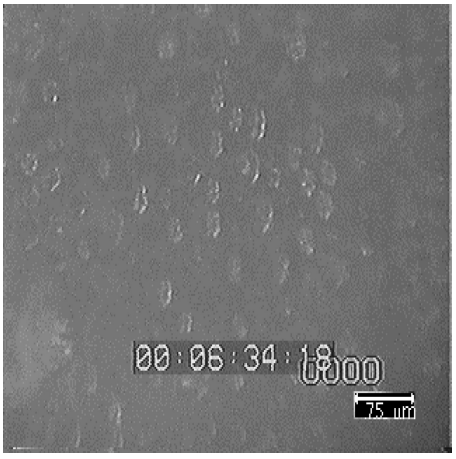

b)

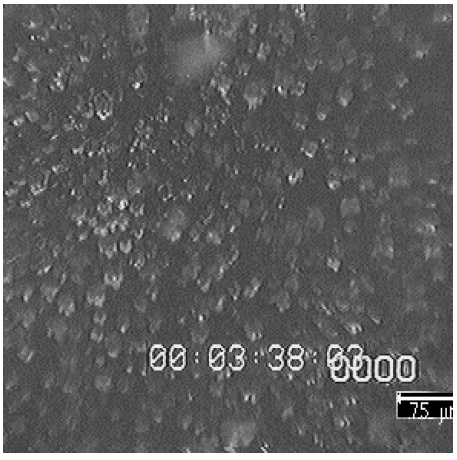

c)

Fig. 8 Early frost growth on PTFE substrate: a)$T_w = -11.0°C$, $T_a = 11.2°C$, $\omega = 0.0050$, $v = 0.93$ m/s, and time ~ 1000 s; b) $T_w = -17.5°C$, $T_a = 11.2°C$, $\omega = 0.0050$, $v = 0.93$ m/s, and time ~ 400 s; and c) $T_w = -25.1°C$, $T_a = 10.5°C$, $\omega = 0.0050$, $v = 0.93$ m/s, and time ~ 210 s.

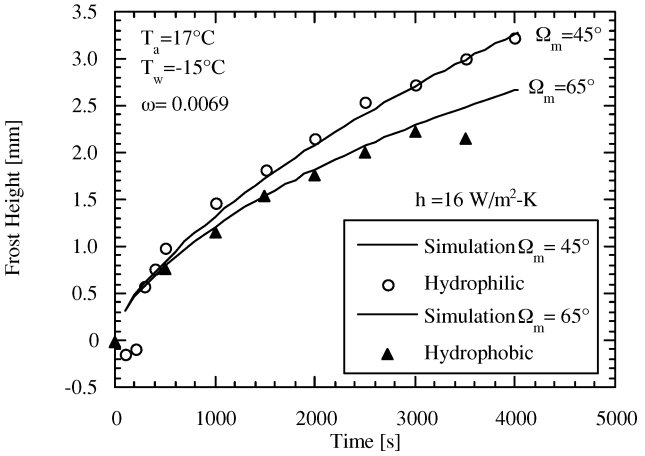

Fig. 9 Frost height vs time on hydrophilic and hydrophobic substrates, v = 1.2 m/s (error in height measurement, ±0.1 mm in mature growth period).

Analysis

The experimental observations clearly show that the density and thickness of frost are not only dependent on the substrate contact angle but that there is a time-dependent variation in growth rate and densification that results in an intersection of both the density and thickness vs time curves for the two substrates (not necessarily occurring simultaneously). The difference in thermal conductivity is caused by a difference in frost structure caused by the distribution of condensate on the substrate before freezing. We hypothesize that the difference between the frost layers grown on a hydrophobic and hydrophilic substrate is caused by the difference in thermal conductivity between the layers. The distribution of condensate determines the locations and number of frost spires. The conductivity of the frost layer is affected by the spacing of these spires. Closer spaced spires result in frost growth that is more normal to the substrate and has a higher effective conductivity. As the frost layer grows and densifies, the effect of the differences in the initial condensation is expected to decrease; however, frost only grows on existing frost, and the foundation of the frost layer influences the resulting structure.

The thermal conductivity of a frost layer growing on a hydrophilic substrate is higher than that of a layer growing on a hydrophobic substrate, and the difference is caused by the distribution of liquid on the substrates at the end of the condensation period. Frost spire densities are higher for hydrophilic substrates than for hydrophobic substrates. Higher conductivity results in a smaller temperature gradient across the frost layer and a lower frost surface temperature. The smaller temperature gradient and lower interfacial temperature causes a larger driving potential for convective heat and mass transfer, and a larger portion of the convected water vapor is deposited on the surface of the frost (increasing the thickness), rather than diffusing into the layer. In the limit of the Biot number of the frost layer, $h\delta_f/k_f$ approaching zero, all of the water vapor will be deposited on the surface of the frost layer. The result of a small Biot number is readily seen by a mass balance at the frost–air interface, as shown in Eq. (1). Note that the water vapor density gradient within the layer is dependent on the temperature gradient if the saturation ratio within the frost layer is assumed to be unity:

$$h_m\left[\omega_\infty - \omega\left(z=\delta_f^+,t\right)\right]\rho_a = D_{\text{eff}}\frac{\partial\rho_v\left(z=\delta_f^-,t\right)}{\partial z} + \rho_f\frac{\mathrm{d}\delta_f}{\mathrm{d}t} \quad (1)$$

To examine the preceding hypothesis quantitatively, the mature growth model proposed by Tao and Besant[13] will be considered. This model is based on the conservation of mass and energy. Initial conditions are acquired by observation of the incipient growth of frost under a scanning confocal microscope. The details of the numerical model will be quickly reviewed for completeness, then explanations of the initial conditions and conductivity are given before the results of the simulation are examined and compared to experiments. A finite difference model is developed and solved explicitly with a 1-s time step and a maximum special step of 0.0004 m. For frost growth on a flat plate, only transport in the direction normal to the plate is considered. The energy and mass conservation within the frost layer yield

$$\rho_f c_p\frac{\partial T}{\partial t} + \dot{m}\lambda_{\text{sg}} = \frac{\partial}{\partial z}\left(k_{\text{eff}}\frac{\partial T}{\partial z}\right) \quad (2)$$

$$\frac{\partial(\varepsilon_a\rho_v)}{\partial t} - \dot{m} = \frac{\partial}{\partial z}\left(D_{\text{eff}}\frac{\partial\rho_v}{\partial z}\right) \quad (3)$$

where the phase change rate is related to the volume fraction by

$$\frac{\partial\varepsilon_b}{\partial t} + \frac{\dot{m}}{\rho_{\text{ice}}} = 0 \quad (4)$$

$$\varepsilon_a + \varepsilon_b = 1 \quad (5)$$

The boundary conditions for the energy conservation equation are a convection condition at the frost surface and an isothermal condition at the plate surface T_w. For the mass balance equation, the boundary conditions are that no mass is transferred into the plate and that there is a convective condition at the frost surface. (With regard to mass, the derivative of the mass concentration must be zero at the substrate surface, $z = 0$.) The vertical growth is computed by Eq. (1), with frost properties assigned in a manner consistent with available experiments. The diffusion of water vapor and densification of the frost layer needs to be quantified. The effective diffusivity is taken as

$$D_{\text{eff}} = \varepsilon_a D_{ab} \quad (6)$$

Tao and Besant[13] used a correlation for the conductivity of frost that depended solely on density and that was developed by Yonko and Sepsy[3]:

$$k_{\text{eff}} = 0.02422 + 7.214\times10^{-4}\rho_f + 1.1797\times10^{-6}\rho_f^2 \quad (7)$$

where ρ_f is in kilograms per cubic meter and k_{eff} is in Watts per meter Kelvin. The conductivity of a porous, fibrous medium such as frost depends inherently on the structure and orientation of the fibers or crystals in this case, as well as the porosity:

$$k_{\text{eff}} = k_{\text{eff}}(\text{structure}, \varepsilon_b) \quad (8)$$

Two limiting cases that elucidate the effect of structure on conductivity are that of two media in series or parallel. For values of porosity typical to frost, the conductivity for these two extreme cases, with air and ice as the heat conducting media, can differ by a factor of 20. The orientation of the frost crystal relative to the macroscopic direction of heat flow Ω determines the effect that the structure has on conductivity:

$$k_{\text{eff}} = k_{\text{eff}}(\Omega, \varepsilon_b) \quad (9)$$

Bauer[14] has proposed an expression for the conductivity of a fibrous media based on porosity and the average orientation of the fibers:

$$1-\varepsilon_b = \left(\frac{k_{\text{eff}}-k_{\text{ice}}}{k_a-k_{\text{ice}}}\right) \times\left(\frac{k_{\text{eff}}+[(1-\sin^2\Omega)/(1+\sin^2\Omega)]k_{\text{ice}}}{k_a+[(1-\sin^2\Omega)/(1+\sin^2\Omega)]k_{\text{ice}}}\right)^{-[\sin^2\Omega/(1+\sin^2\Omega)]} \quad (10)$$

for fibers parallel to the macroscopic direction of heat flow $\Omega = 0$, and for fibers perpendicular to the macroscopic direction of heat flow $\Omega = 90$ deg. The value of conductivity predicted by Eq. (7) for a frost density between 50 and 500 kg/m^3 is within 1.5% of the value predicted by Eq. (10) with the average ice crystal orientation set at

$\Omega = 53$ deg. This agreement indicates that the frost conductivity can be approximated by an average crystal orientation more parallel to the substrate than perpendicular to it.

Single crystal growth has been systematically analyzed and found to depend on crystal temperature and degree of supersaturation. Frost, however, is a complex, polycrystalline material with properties dependent on local heat and mass transfer as well as surface kinetics. The proximity of neighboring crystals can affect the availability of water vapor and the direction of crystal growth; this proximity of crystals is the mechanism by which the substrate contact angle affects frost properties. For the hydrophobic substrate, there is a relatively large distance between crystals growing up from the substrate, which is a condition favorable to horizontal crystal growth along the vapor pressure gradient between crystals, thus, filling the layer with crystals oriented parallel to the substrate. For a hydrophilic substrate, the spacing between vertical spires is smaller, not limited by the location of frozen droplets because there is a frozen layer covering the substrate. The crystal growth, therefore, is predominantly normal to the substrate.

In the early growth period, the orientation of crystals is observed to be predominantly normal to the substrate, and a value for the average crystal orientation closer to zero is adopted, $\Omega_i = 25$ deg. (The conductivity is a weak function of fiber orientation below 25 deg.) As the crystal layer grows and becomes multifaceted, the average orientation of the crystals approaches that of the mature frost layer. The following equation is proposed to model this evolution

$$\Omega = (\Omega_m - \Omega_i)[1 - \exp(-\sqrt{\tau}/0.1)] + \Omega_i \tag{11}$$

where Ω_m and Ω_i are the mature and initial average crystal orientations, respectively, and τ is the environmental time proposed by Storey and Jacobi.[15] The exponential form of this equation provides a smooth transition from the structure encountered in the early growth period to that expected in the mature growth period. The time constant of 0.1 is chosen on the basis of observations of the time necessary for transition from the early growth period to the mature growth period.[15]

The early frost growth period also differs from the mature growth period in terms of the number of possible locations for water vapor deposition. Microscopy reveals that the initial volume fraction of frost appearing from the frozen condensate is relatively low. Water vapor is deposited directly onto existing frost, and so the increase in height between time steps of the model maintains this low density (after the condensate has frozen water vapor deposits onto the frozen crystals not onto the substrate). The deposition of water vapor onto the frost layer is most intense during the early growth period because the driving potential between the freestream and the frost surface is the highest. The low frost density and high deposition rate accounts for the fast growth rate during the early growth period.

The equation used to compute the volume fraction of the new frost layer is similar to the matching equation for crystal orientation. It is given by

$$\varepsilon_b = (\varepsilon_{bm} - \varepsilon_{bi})[1 - \exp(-\sqrt{\tau}/0.1)] + \varepsilon_{bi} \tag{12}$$

where ε_{bi} and ε_{bm} are the early and mature growth density used to compute the new growth on the frost layer. On the basis of experimental observations, as well as those made by Tao and Besant,[13] a value of 0.02 is proposed for ε_{bi} and a value of 0.12 for ε_{bm}.

Although the frost growth was simulated, the average value of crystal orientation Ω_m was adjusted to fit the observed trends. Other than the initial conditions, this was the only parameter changed from the hydrophilic to hydrophobic simulation. The value of Ω_m is 45 deg for a hydrophilic substrate and 65 deg for a hydrophobic substrate. The simulated frost thickness is plotted along with the experimental data in Fig. 9. The temporal axis for the hydrophobic data has been offset by 500 s to account for the long condensation period. The simulated density is approximately 20% less than that determined experimentally. The density of frost on the hydrophilic substrate starts higher than that on the hydrophobic substrate because it is set that way for the initial condition of the model; however, at the end of the simulation, the density on the hydrophilic substrate is 12% lower than that on the hydrophobic substrate. Recall that the experimental results revealed a 14% difference in the densities.

Extension to Substrate Surface Temperature/Conductivity Dependence

As reported in the literature pertaining to frost, the conductivity of the frost layer is usually correlated to frost density.[16,17] Of course, this is a correlation of convenience because it has been difficult to examine the conductivity of frost as a function of structure. This correlation is obviously erroneous when the conductivity of frost is calculated as a function of substrate contact angle because the lower-density frost found on a hydrophilic substrate has a higher conductivity than that found growing on a hydrophobic substrate under identical environmental conditions. Likewise, frost growing at a lower substrate temperature has a higher conductivity and lower density.[18] The higher conductivity and lower frost density at lower substrate temperatures is readily seen by examination of the curve fits proposed by Mao et al.[18] The density change with plate temperature and time is given as

$$\rho \propto \left(\frac{T_{\text{tp}} - T_w}{T_a - T_w}\right)^{-0.728} t^{0.147} = T^{*-0.728} t^{0.147} \tag{13}$$

and the conductivity changes as

$$k \propto \left(\frac{T_{\text{tp}} - T_w}{T_a - T_w}\right)^{0.901} t^{0.791} = T^{*0.901} t^{0.791} \tag{14}$$

where $0.24 < T^* < 0.51$. The conductivity of the frost layer was determined under the assumption that the frost surface temperature was at the triple point of water. As an example, take T^* to be 0.30 and 0.45 for two different substrate temperatures, with all other conditions held constant. The density at any given time on the colder substrate, $T^* = 0.45$, is 74% of that on the warmer substrate, $T^* = 0.30$, and the conductivity of the frost is 44% greater on the colder substrate than on the warmer.

Although the characteristics of crystal growth have been reported to be a function of temperature and supersaturation,[1] the measurements of these reports were conducted on crystals that were not competing for water vapor. The growth of crystals growing in a frost layer is constrained by temperature and the availability of water vapor. Because of this constraint, crystals growth occurs along the vapor pressure gradient. As hypothesized, the substrate has the effect on frost properties that the smaller, closer-spaced droplets seen on a colder substrate foster the development of a frost layer with a higher conductivity. This higher conductivity is predominantly caused by frost growth normal to the substrate.

Condensation Period

The foregoing observations and analysis indicate that the distribution of condensate at the time of freezing is a major determinant of mature frost properties. It is desirable to understand the parameters affecting the duration of the condensation period because droplet size and distribution are a function of the quantity of liquid on the substrate and, therefore, the duration of the condensation period. Nucleation is a stochastic process, and predicting the duration of the condensation period is difficult; however, there are definite trends (see Ref. 2). From nucleation theory, the heterogeneous ice nucleation rate J is given by

$$J(T) = A \exp(B/T) \tag{15}$$

where A and B are constants that depend on the nucleation site characteristics.[1] The probability P that freezing will occur in a given time interval is[1]

$$P(V, t) = 1 - \exp\left[-\int_0^t VJ(T)\,\mathrm{d}t\right] \tag{16}$$

The probability that the water will freeze increases significantly as the temperature of the substrate decreases, resulting in short condensation periods. The probability of freezing also increases with

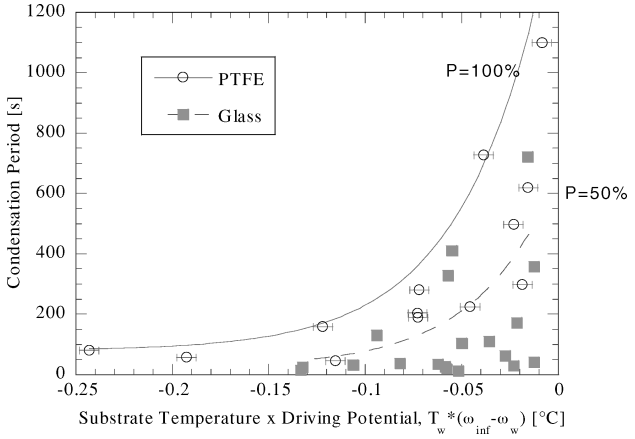

Fig. 10 Condensation period vs substrate temperature times mass transfer driving potential (error bars for PFTE representative of glass, error in condensation period ±1 s).

an increase in the amount of water on the substrate. (The number of possible heterogeneous nucleation sites increases with the increase of water volume.) The substrate also influences the condensation period in two ways, either or both of which may occur: 1) Droplets on a hydrophilic substrate have greater contact with the substrate, exposing the droplet to a greater number of heterogeneous nucleation sites located on the substrate, altering the magnitude of the parameter *A*. 2) The heterogeneous nucleation sites on a hydrophilic substrate may require less activation energy to form a viable ice nucleus than those on a hydrophobic substrate, resulting in a modification of the parameters *A* and *B* in Eq. (15). In Fig. 10, the length of the condensation period plotted vs the substrate temperature, multiplied by the mass transfer driving potential, is shown. (The absolute humidity difference is approximately proportional to the amount of water on the substrate at a given time.) As expected, the condensation period is shorter at lower substrate temperatures and higher mass transfer driving potentials. The mass of condensate on the substrate was not measured but inferred through the driving potential. Therefore, the effect of mass on the substrate and the effect of the deposition rate could not be separated. The condensation period is also shorter for water condensing on the hydrophilic substrate than on the hydrophobic.

It is apparent that accurate prediction of the duration of the condensation period is difficult because of the stochastic nature of nucleation. However, given the duration of the condensation period and the substrate contact angle, along with the environmental parameters, it is possible to predict the distribution of condensate (see Ref. 2).

Summary

The mature growth and densification of a frost layer has been shown to be dependent on the local distribution of frozen water within the frost layer. Because frosting at moderate subcooling begins as condensation, the substrate wettability affects the growth and densification of the frost layer. Experiments conducted on a hydrophobic and hydrophilic substrate showed that at the end of the condensation period, the condensate/ice coverage of the substrate surface was 34 and 86%, respectively. The thickness of the condensate/ice on the hydrophobic substrate was twice that on the hydrophilic substrate, whereas the density of the condensate/ice was 42% of that on the hydrophilic substrate. For a hydrophobic substrate, the number and location of frost spires has been shown to be dependent on the condensate distribution, varying from approximately 30 to more than 200 (in the field of view of the microscope), in direct correlation to the number of droplets on the substrate at the end of the condensation period. The mature frost layer that develops on the hydrophilic substrate after more than an hour of growth was found to have a thickness that was 23% higher than the frost layer on the hydrophobic substrate, whereas the density of the frost layer was 14% less than that on the hydrophobic layer.

The trends observed for the density (or mass deposited) and thickness of frost as a function of substrate are hypothesized to be caused by a difference in the thermal conductivity of the frost layers. Even though the mature frost layer on the hydrophilic substrate was thicker than that on the hydrophobic substrate, the layer was found to be less dense. Therefore, for the hydrophobic layer, there is a larger quantity per unit volume of the high conductivity material, ice. Yet, the conductivity of this frost layer is less than the layer of lower density frost on the hydrophilic substrate. The difference in conductivity between the frost layers is caused by the orientation of frost spires within the layer. Condensate distribution has been shown to affect the number and orientation of these spires in the early frost growth period. Therefore, the condensate distribution affects the structure of the frost layer. A correlation for the conductivity of a fibrous material based on structure has been implemented in a numerical model for frost growth to determine if a change in the thermal conductivity of the frost layer could affect the observed differences in thickness and density. The trends of thickness and density observed for mature frost growth are predicted by the model, with the only variable being the average orientation of the crystals. The initial conditions on the hydrophobic and hydrophilic substrate are commensurate with observations. The hypothesis that the conductivity is affected by the distribution of condensate is also bolstered by the trends observed for the condensate distribution and conductivity of the frost layer as a function of substrate temperature.

One implication of this work is that frost properties can be manipulated by alteration of the condensate distribution. Although substrate contact angle is an obvious means of manipulating the distribution, environmental parameters (during the condensation period) can also be used to affect the distribution of condensate and the subsequent frost properties. For example, alteration of the transient temperature profile (during the cooldown period), the heat/mass transfer coefficient (air velocity and geometry), and humidity ratio can all affect the quantity of condensate and number of droplets on the substrate, as well as the duration of the condensation period.

References

[1]Hobbs, P. V., *Ice Physics*, Clarendon, Oxford, England, U.K., 1974.

[2]Hoke, J. L., Georgiadis, J. G., and Jacobi, A. M., "The Interaction Between the Substrate and Frost Layer Through Condensate Distribution," Dept. of Mechanical Engineering, Air Conditioning and Refrigeration Center, Univ. of Illinois at Urbana–Champaign, Rept. ACRC TR-177, Urbana, IL, 2000.

[3]Yonko, J. D., and Sepsy, C. F., "An Investigation of the Thermal Conductivity of Frost While Forming on a Flat Horizontal Plate," *ASHRAE Transactions*, Vol. 73, No. 2, 1967, pp. I.1.1–I.1.10.

[4]Hayashi, Y., Aoki, A., Adachi, S., and Hori, K., "Study of Frost Properties Correlating with Frost Formation Types," *Journal of Heat Transfer*, Vol. 99, May 1977, pp. 239–245.

[5]Tao, Y.-X., Besant, R. W., and Mao, Y., "Characteristics of Frost Growth on a Flat Plate During the Early Growth Period," *ASHRAE Transactions*, Vol. 99, No. 1, 1993, pp. 746–753.

[6]Sahin, A. Z., "An Analytical Study of Frost Nucleation and Growth During the Crystal Growth Period," *Warme- und Stoffubertragung*, Vol. 30, No. 5, 1995, pp. 321–330.

[7]O'Neal, D. L., and Tree, D. R., "Measurement of Frost Growth and Density in a Parallel Plate Geometry," *ASHRAE Transactions*, Vol. 90, No. 2A, 1984, pp. 278–290.

[8]Padki, M. M., Sheirf, S. A., and Nelson, R. M., "A Simple Method for Modeling the Frost Formation Phenomenon in Different Geometrics," *ASHRAE Transactions*, Vol. 95, No. 2, 1989, pp. 1127–1137.

[9]Georgiadis, J. G., "Microscopic Study of Frost Inception," *Proceedings of the 2nd European Thermal-Sciences Conference*, edited by C. P. Celata, P. DiMarco, and A. Mariani, Edizioni EDS, Pisa, Italy, 1996, pp. 269–277.

[10]Dyer, J. M., Storey, B. D., Hoke, J. L., Jacobi, A. M., and Georgiadis, J. G., "An Experimental Investigation of the Effect of Hydrophobicity on the Rate of Frost Growth in Laminar Channel Flows," *ASHRAE Transactions*, Vol. 106, No. 1, 2000, pp. 143–151.

[11]Seki, N., Fukusako, S., Matsuo, K., and Uemura, S., "Incipient Phenomena of Frost Formation," *Bulletin of the Japanese Society of Mechanical Engineering*, Vol. 27, No. 233, 1984, pp. 2476–2482.

[12]Georgiadis, J. G., Hoke, J. L., and Ramaswamy, M., "Quantitative Visulatization of Early Frost Growth via Scanning Confocal Microscopy," *International Journal of Heat and Mass Transfer* (submitted for publication).

[13]Tao, Y.-X., and Besant, R. W., "Prediction of Spatial and Temporal Distributions of Frost Growth on a Flat Plate Under Forced Convection," *Journal of Heat Transfer*, Vol. 115, No. 2, 1993, pp. 278–281.

[14]Bauer, T. H., "A General Analytical Approach Toward the Thermal Conductivity of Porous Media," *International Journal of Heat and Mass Transfer*, Vol. 36, No. 17, 1993, pp. 4181–4191.

[15]Storey, B. D., and Jacobi, A. M., "The Effect of Streamwise Vortices on the Frost Growth Rate in Developing Laminar Channel Flows," *International Journal of Heat and Mass Transfer*, Vol. 42, No. 20, 1999, pp. 3787–3802.

[16]Ostin, R., and Andersson, S., "Frost Growth Parameter in a Forced Air Stream," *International Journal of Heat and Mass Transfer*, Vol. 34, Nos. 4–5, 1991, pp. 1009–1017.

[17]Sahin, A. Z., "An Experimental Study on the Initiation and Growth of Frost Formation on a Horizontal Plate," *Experimental Heat Transfer*, Vol. 7, No. 2, 1994, pp. 101–119.

[18]Mao, Y., Besant, R. W., and Falk, J., "Measurement and Correlations of Frost Properties with Laminar Airflow at Room Temperature over a Flat Plate," *ASHRAE Transactions*, Vol. 99, No. 1, 1993, pp. 739–745.